XAFS investigation of $[Pd(NH_3)_4][AuCl_4]_2$ and its thermolysis products

Tatiana Nedoseykina · Pavel Plyusnin · Yuri Shubin · Sergey Korenev

Abstract Thermolysis of double complex salt $[Pd(NH_3)_4][AuCl_4]_2$ has been studied in helium atmosphere from ambient to 350 °C. The XAFS of Pd K and Au L_3 edges and thermogravimetry measurements have been carried out to characterize the intermediates and the final product. In the temperature range 115–160 °C the complex is decomposed to form $Pd(NH_3)_2Cl_2$ and $AuCl_{4-x}N_x$ species with x ranging from 2 to 3. Subsequent heating of the intermediate up to 300 °C leads to the total loss of NH_3. The Au–Cl and Au–Au bonds form the local environment of Au at the stage of decomposition while only four chlorine atoms are around Pd. At the temperature of 330 °C the Au and Pd nanoparticles as well as residues of palladium chloride are detected. The final product consists of separated Au and Pd nanoparticles.

Keywords Thermolysis · TG · XAFS · Double complex salts · Nanoparticles

Introduction

In recent years a great deal of attention has been paid to double complex salts because of their promising application as precursors for preparation of bimetallic nanoparticles through the thermal decomposition of these salts [1–5]. The salts have a general formula $[M_1A_n]_x[M_2B_m]_y$, where M_1 and M_2 are central metal atoms in the complex cation and anion, respectively, A and B are the ligands. This kind of distribution of the metal atoms in the precursor may

T. Nedoseykina (✉) · P. Plyusnin · Y. Shubin · S. Korenev
Nikolaev Institute of Inorganic Chemistry SB RAS, 3, Acad.
Lavrentiev Ave, Novosibirsk, Russia 630090
e-mail: tatianani@list.ru

allow preparing single-phase solid solution of different composition. The composition can be easily controlled by a stoichiometry of the complex precursor. For these reasons the use of bimetallic molecular clusters as precursors is considered an attractive alternative to convenient synthesis methods of bimetallic nanoparticles in Catalysis [6–8]. Other well-crystallized complex salts such as oxalates, tartrates, and citrates yield mixed oxides on thermal decomposition at moderate temperatures [9, 10]. Thermal decomposition is conventional and often used method for preparing nanoparticles [1–5, 11–16].

The investigation of $[Pd(NH_3)_4][AuCl_4]_2$ thermolysis [16] revealed a dependence of final product on the heating rate and atmosphere of decomposition. In hydrogen atmosphere two-phase product $Pd_{0.3}Au_{0.6}$ and Pd and single-phase product $Pd_{0.33}Au_{0.66}$ are obtained at the heating rate of 30 °C/min and 15 °C/min, respectively. The decomposition of the complex in the air and helium atmospheres results in formation of monometallic particles Pd and Au. In spite of many investigations on the double complex salts [2–5, 16] the formation mechanism of bimetallic and monometallic nanoparticles has not yet been elucidated to understand the preparative technique for the control of the particles size and composition. The limited understanding of these mechanisms deals with, in large part, the difficulty of characterizing intermediates because they are often amorphous. XAFS spectroscopy is a unique method that allows the determination of structure in amorphous as well crystalline materials. This method includes two techniques XANES (X-ray Absorption Near Edge Structure) and EXAFS (Extended X-ray Absorption Fine Structure) [17, 18]. XANES spectra provide information about vacant orbitals, oxidation state, and site symmetry of the X-ray-excited atoms while EXAFS spectra yield information on the interatomic distances,

variation in the distances (i.e., Debye-Waller factors), the identity and number of nearest neighboring atoms (coordination numbers) within the first few coordination shells of the absorption atom.

In this article we present Au L_3 and Pd K-edges XAFS investigation of the $[Pd(NH_3)_4][AuCl_4]_2$ and its intermediate products of thermolysis carried out in the helium atmosphere to enlighten on the thermolysis of this double complex salt and hence on the formation mechanism of metallic nanoparticles.

Experimental

Initial compounds for a synthesis of the double complex salt $[Pd(NH_3)_4][AuCl_4]_2$ were $[Pd(NH_3)_4]Cl_2$, $[Pd(NH_3)_4]$ $(NO_3)_2$ and $H[AuCl_4]$. First $[Pd(NH_3)_4]Cl_2$ was synthesized by procedure described in [19]. Then this compound was used to prepare $[Pd(NH_3)_4](NO_3)_2$ by a substitution of chloride ion for nitrate ion. Solution $H[AuCl_4]$ was obtained by dissolving of gold (99.99%) in aqua regia and subsequent boiling down in water and hydrochloric acid.

A required quantity of the solution of $H[AuCl_4]$ (1.0 mol/l) and saturated aqueous solution of $[Pd(NH_3)_4]$ $(NO_3)_2$ (0.3 mol/l) were mixed. It immediately led to a formation of crystalline precipitation in the form of yellow needles. The obtained precipitate was filtered off under vacuum and subsequently washed with minimal quantity of water, methanol and then air-dried. The yield of $[Pd(NH_3)_4][AuCl_4]_2$ was about 90%.

Thermogravimetric (TG) measurements were carried out on a Q-1000 derivatograph. A test portion of $[Pd(NH_3)_4][AuCl_4]_2$ was put in a quartz crucible and heated with the rate of 10 °C/min in a helium flow (150 ml/min). Differential thermal analysis (DTA) was carried out on an STA 409 PC Luxx® (NETZSCH) in the helium atmosphere with the heating rate of 5 °C/min.

XAFS spectra at Au L_3 and Pd K edges of the double complex salt and its products of thermolysis were recorded at the 7C1 Electrochemistry beamline at PAL (Pohang Accelerator laboratory, Republic of Korea) with ring current of 120–170 mA at 2.0 GeV. A Si (111) double-crystal monochromator with an energy resolution $\Delta E/E = 2 \times 10^{-4}$ was used. The data acquisition system for XAFS comprised three ionization detectors measuring beam intensity of incidence I_0, transmitted I_t, and transmitted through reference I_r. The reference channel was employed primarily for internal calibration of the edge positions by using pure metal foils. All chambers were filled by nitrogen. XAFS spectra recorded in the transition mode were analyzed and presented here for all the samples. XAFS data were analyzed by IFFEFIT software package [20, 21].

Fourier transformation (Δk) and fit (ΔR) ranges are presented in Table 1 together with the best fits of EXAFS data.

Results and discussion

The TG and DTA results of $[Pd(NH_3)_4][AuCl_4]_2$ presented in Fig. 1 demonstrate three stages of the decomposition at 115–160 °C, 200–290 °C, and 290–330 °C, respectively. The first stage is accompanied by endoeffect but without a mass loss. During this stage the compound changes color from yellow to dark brown. The second and third stages of the thermolysis are poorly resolved and accompanied by exothermic and endothermic effects, respectively. The complex is fully decomposed at 350 °C. For XAFS investigation, the intermediates were chosen at the thermolysis temperatures of 190 (intermediate 1), 300 (intermediate 2) and 330 °C (intermediate 3). The final product was taken at 350 °C.

The Au L_3 and Pd K edges XANES spectra of the initial complex and its intermediates and the final product of the thermolysis are depicted in Fig. 2. In the Pd K-edge XANES spectra the absorption threshold, called the white line, corresponds to the 1s-4p electron transitions. It is well known that the intensity and position of the white line are sensitive to the changes in the electronic occupancy in the valence orbital and ligand field environments of the absorbers. Hence, it can be used to estimate the density of the unoccupied states and the variation in the oxidation state of the Pd absorber. As it is seen from Fig. 2a, the white line is slightly decreased in intensity and broadened as the thermolysis temperature increases from ambient to 300 °C. At the same time, for these spectra no shift of the white line position is observed. All of these indicate on the unchangeable Pd oxidation state and changes in the local environment of the Pd^{2+}. In the $[Pd(NH_3)_4][AuCl_4]_2$ complex, the geometry around Pd^{2+} is square planar. The average Pd–N distance is 2.043 Å [16]. For intermediate 2 the XANES spectrum is the closest similar to that of $(NH_4)_2PdCl_4$ [22], where the Pd atoms are surrounded by four chlorine atoms. The Pd spectrum of intermediate 1 looks like the interstitial between the spectra of the initial complex and intermediate 2. So it can suggest that the local environment of Pd^{2+} consists of two N and two Cl atoms. The Pd spectra of intermediate 3 and final product resemble well to that of the Pd metal foil.

The white line of the Au L_3-edge XANES spectra is due to the 2p-5d electron transitions and gradually decreases in intensity going from the initial complex to intermediates 1 and 2 (Fig. 2b). In the Au spectrum of intermediate 2, the edge position shifts slightly to higher energy and a peak at 11947 eV appears. This peak is typical of the bulk Au foil.

Table 1 EXAFS parameters for [Pd(NH$_3$)$_4$][AuCl$_4$]$_2$ and its thermolysis products

$T/°C$	Bonds	CN	$R/Å$	$\sigma^2/Å^2$	$\Delta E_0/eV$	S_0^2	$C_3/Å^3$	$C_4/Å^4$	$F/\%$	$\Delta k/Å^{-1}$ $\Delta R/Å$
24	Pd–N	2.0(1)	2.046(7)	0.0021(9)	0.5(9)	0.8			1.0	2.5–10.0
	Pd–N	2.0(1)	2.054(7)							1.0–2.2
	Au–Cl	4.0(1)	2.284(7)	0.0021(3)	10(1)	0.8			0.9	3.1–14
										1.0–2.4
190	Pd–N	2.0(3)	2.041(3)	0.002(2)	6.7(6)	0.8			0.2	2.9–12.0
	Pd–Cl	2.0(3)	2.334(6)	0.0013(8)						1.0–2.4
	Au–N	1.4(3)	2.029(9)	0.002(2)	10(1)	0.8			0.9	2.8–14.0
	Au–Cl	2.6(6)	2.285(8)	0.0013(5)						1.0–2.4
300	Pd–Cl	3.8(4)	2.315(9)	0.003(1)	3.5(7)	0.8			0.3	3.0–12.0
										1.0–2.4
	Au–Cl	2.2(3)	2.283(7)	0.001(1)	9(1)	0.8			1.1	2.8–12.0
	Au–Au	3(1)	2.89(2)	0.006(3)						1.0–3.3
330	Pd–Cl	1.2(3)	2.290(9)	0.002(1)	0.0(3)	0.6	$1(1)*10^{-4}$		1.7	2.9–12.0
	Pd–Pd	11.0(5)	2.750(3)	0.0067(2)						1.5–5.5
	Pd–Pd	5.6(2)	3.889(4)	0.010(3)						
	Pd–Pd	2.5(9)	4.764(4)	0.0083(8)						
	Au–Au	11.8(6)	2.879(5)	0.010(1)	5.8(4)		$2.6(8)*10^{-4}$			2.8–12.5
	Au–Au	5.9(3)	4.072(7)	0.012(1)				$5(3)*10^{-5}$		1.8–6.0
	Au–Au	24(1)	4.988(8)	0.013(2)		0.6			0.9	
350	Pd–Pd	12.0(4)	2.750(4)	0.0048(2)	2.1(4)	0.6	$1.2(5)*10^{-4}$		0.6	2.9–12.0
	Pd–Pd	6.0(2)	3.890(5)	0.0082(3)						1.0–5.5
	Pd–Pd	24.0(6)	4.764(7)	0.0085(3)						
	Au–Au	11.8(3)	2.882(7)	0.0096(1)	6.0(3)	0.6	$2.5(7)*10^{-4}$		0.6	2.8–12.0
	Au–Au	5.9(2)	4.075(9)	0.012(2)				$5(2)*10^{-5}$		1.9–5.6
	Au–Au	23.5(6)	4.991(1)	0.013(1)						

CN coordination number, R interatomic distance, σ^2 Debye-Waller factor, ΔE_0 correction of the absorption edge position, S_0^2 electron amplitude reduction factor, C_3 and C_4 are the third and forth cumulants (a measure of the deviation of Pair Distribution Function from the Gaussian shape [17, 18]), F quality of the fit (characterizes differences between theoretical and experimental data [17]), Δk Fourier transformation range, and ΔR fit range
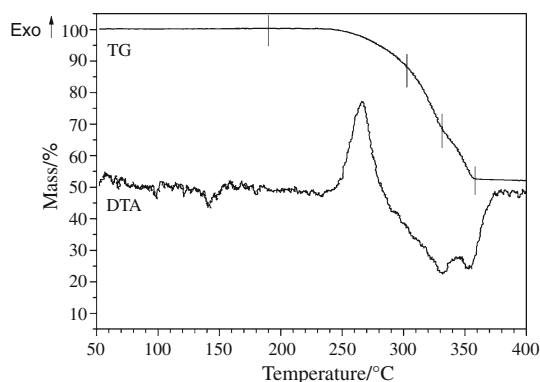

Fig. 1 TG and DTA curves of [Pd(NH$_3$)$_4$][AuCl$_4$]$_2$. *Vertical bars* show the temperatures at which the products were chosen for the study

Here, it is necessary to remind that the Au L$_3$ edge position shifts to the higher energy as far as the Au oxidation state changes from Au^{3+} to Au^0 and Au^{1+}. The unusual shift of the edge position for Au^{3+} is ascribed to an intensive and poorly resolved pre-edge peak [23]. Thus, at the temperature of 300 °C, it occurs as a partial reduction of Au^{3+} to Au^0. The Au spectra of intermediate 3 and final product are similar to that of the Au metal foil indicating the formation of the gold particles.

The Fourier transformed (FT) EXAFS spectra at the Au L$_3$ (Au-FT) and Pd K edges (Pd-FT) are shown in Fig. 3. For the initial complex a single peak at 1.5 Å in the Pd-FT and at 1.9 Å in the Au-FT is attributed to Pd–N and Au–Cl coordination shell, respectively. By increasing the thermolysis temperature to 190 °C, the Pd-FT and Au-FT show the peak with maximum at 1.9 Å and a shoulder at 1.6 Å. Additionally, the Au-FT peak decreases in magnitude. It can be ascribed to the decrease in the number of Cl atoms and/or appearance of N atoms in the first coordination shell of Au. The shoulder of the Pd-FT peak agrees with the Pd–N peak of the initial DCS. All of these might suggest a model where Pd and Au atoms are surrounded by nitrogen

Fig. 2 Pd K (**a**) and Au L$_3$ (**b**) edges XANES of the initial complex and its thermolysis products
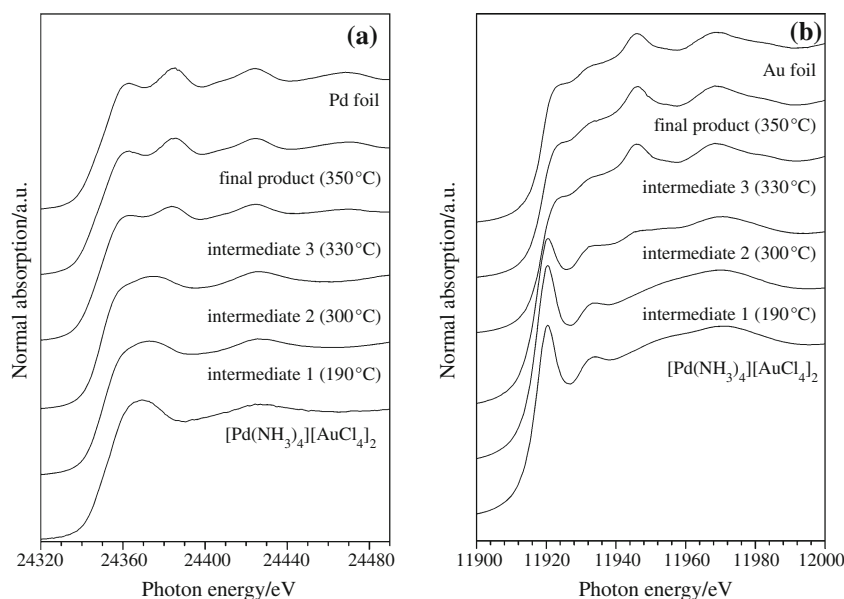
Fig. 3 Fourier transformations of experimental $k^2\chi(k)$ Pd K and Au L$_3$ edges EXAFS (*solid curves*) and fits (*dots curves*) of the initial complex and its thermolysis products. Here, r is the interatomic distance to within the phase-shift correction (δ)
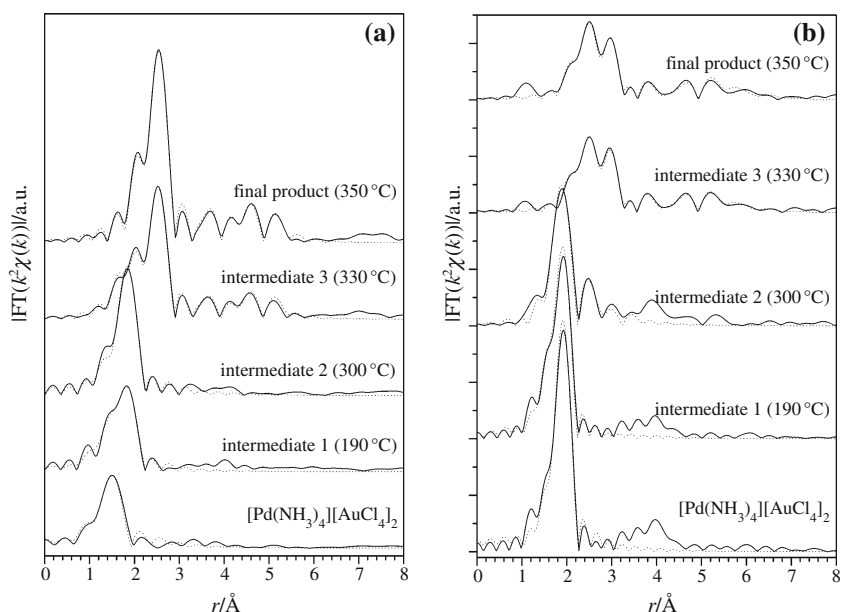
and chlorine atoms. The use of such model as the initial one in the fitting procedure of the EXAFS spectrum gives a good result (Table 1). Indeed, the first coordination shell of Pd consists of two N and two Cl atoms at distances 2.04 and 2.33 Å, respectively. In the first coordination shell of Au, 1.4 Cl and 2.6 N atoms are found at distances 2.03 and 2.29 Å, respectively. As it was assumed in [16], the intermediate of the thermolysis stage consists of amorphous compounds Pd(NH$_3$)$_2$Cl$_2$ and Au(NH$_3$)Cl$_3$. This assumption is mainly confirmed by both XANES and EXAFS. However, the obtained coordination numbers (*CN*) for Au–N and Au–Cl indicate a coexistence of the Au(NH$_3$)Cl$_3$ and Au(NH$_3$)$_2$Cl$_2$ phases.

Main peak at 1.9 Å is observed in the Pd-FT and Au-FT of intermediate 2. From the fitting procedure of Pd K and Au L$_3$ edges EXAFS spectra it was found that this peak corresponds to a coordination shell consisting of chlorine atoms. For the best fit of the Au L$_3$-edge EXAFS for this intermediate, the contribution from Au-Au was taken into account. Thus, there are two chlorine atoms at 2.28 Å and three gold atoms at 2.89 Å in the local environment of Au.

As mentioned above, the XANES spectra of both the Au L$_3$ and Pd K edges for intermediate 3 and final product are similar to those of the corresponding metal foils. However, the Au- and Pd-FTs show a reduced magnitude of all peaks compared to those of the corresponding metal foils, i.e., the

reduced amplitude of EXAFS oscillations. It can be caused by a strong disorder in material, particles size and thickness effect [24]. In our research, intermediate 3 and final product were also studied by XRD. Additionally, TEM (transmission electron microscopy) was used to estimate size of particles in the final product. (XRD and TEM data are not shown). The estimation of particles size by both methods gave around 10 and 20 nm for Pd and Au particles, respectively. In this case, the coordination number of the first shell around Au and Pd should be 12 atoms. We measured EXAFS spectrum of Pd metal powder and revealed that the spectrum also has the reduced amplitude of EXAFS oscillations. The reasonable coordination numbers ($CN = 12$) can be obtained only if parameter S_0^2, electron amplitude reduction factor, decreases up to 0.6. Using this sample as a reference for the last products of the thermolysis, the EXAFS parameters were found for them (Table 1). We consider in our case the thickness is the main effect determining the decrease in the EXAFS amplitude.

Discussion of thermolysis formation of metallic nanoparticles

Thermolysis of the double complex salt, [Pd(NH$_3$)$_4$][AuCl$_4$]$_2$, carried out in helium atmosphere from ambient to 350 °C results in the reduction of Au^{3+} and Pd^{2+} to their zero-valent metal nanoparticles. This process starts from a ligand exchange between complex cation and anion of the initial complex. The Au L$_3$ and Pd K edges XANES spectra of intermediate 1, having no significant changes as compared with the initial complex, indicate that the oxidation states of Au and Pd remain to be 3 and 2, respectively. The EXAFS data (Table 1 and Fig. 2) show variations in the identity and number of the nearest neighboring atoms around Pd and Au atoms in intermediate 1 (190 °C). The found coordination number of Au–Cl (2.6) and Au–N (1.4) indicates the total or partial transformation of AuCl$_4^-$ to AuCl$_{4-x}$(NH$_3$)$_x^-$ species with x ranging from 2 to 3. The larger value of CN of Au–Cl might be explained by the domination of the AuCl$_3$(NH$_3$)$^-$ species in the intermediate. The coordination numbers of Pd–N and Pd–Cl match well to these of Pd(NH$_3$)$_2$Cl$_2$. Besides the observed ligand exchange, there is also a partial loss of NH$_3$ by the initial complex. The total loss of the ammonia molecules happens at the temperature higher than 300 °C. At the decomposition temperature of 300 °C, the contribution of the Au–Cl bond still remains dominant though its coordination number decreases down to 2.2 and CN of Au–Au metallic bond increases up to 3. Taking into account the CN for Au–Cl and described above peculiarities in the Au L$_3$-XANES spectrum for intermediate 2, we think that the Au^0 and Au^{1+} are main states presented in this intermediate. Some amount of Au^{3+} is also possible. Thus, the Au particles

formation concurrently occurs with association of Au^0 atoms when the reduction of Au^{1+} species to Au^0 atoms proceeds and finishes at the temperature of 330 °C. The formation of Pd particles is going through the reduction of Pd^{2+} to Pd^0 and finishes at 350 °C.

The obtained final product consisting of monometallic Pd and Au particles is probably due to that the Pd and Au atoms nucleate at different temperatures. The latter originates from Pd and Au species formed at the first stage (Pd(NH$_3$)$_2$Cl$_2$ and AuCl$_{4-x}$N$_x$ species). Thus, for the preparing of bimetallic nanoparticles, the first stage should be suppressed. It can be done by changing the decomposition atmosphere from inert to reduction one. Thermal decomposition of [Pd(NH$_3$)$_4$][AuCl$_4$]$_2$ in hydrogen atmosphere is under study.

Conclusions

The intermediates and final product of the thermolysis of [Pd(NH$_3$)$_4$][AuCl$_4$]$_2$ were studied by the Au L$_3$ and Pd K edges XAFS. Main stages of the thermal decomposition of the complex can be described as following. On the first stage, ligands rearrangement and breakdown of the complex happen. The second stage is characterized by the total loss of NH$_3$ ligands and beginning of the Au-nanoparticles formation. The product of the third stage consists of the Au and Pd nanoparticles as well as residues of palladium chloride. Separated Au and Pd particles form the final product of the thermolysis at the temperature of 350 °C.

References

1. Korenev SV, Venediktov AB, Shubin YV, Gromilov SA, Yusenko KV. Synthesis and structure of binary complexes of platinum group metals—precursors of metallic materials. J Struct Chem. 2003;44:46–59.
2. Shubin YV, Filatov EY, Baidina IA. Synthesis of [M(NH3)5Cl](ReO4)2 (M = Cr, Co, Ru, Rh, Ir) and investigation of thermolysis products. Crystal structure of [Rh(NH3)5Cl](ReO4)2. J Struct Chem. 2006;47:1103–10.
3. Shubin YV, Zadesenets AV, Venediktov AB. Double complex salts [M(NH3)5Cl][M′Br4] (M = Rh, Ir, Co, Cr, Ru; M′ = Pt, Pd): synthesis, X-ray diffraction characterization, and thermal properties. Russ J Inorg Chem. 2006;51:202–9.
4. Zadesenets AV, Venediktov AB, Shubin YV. [Zn(NH3)4][PtCl6] and [Cd(NH3)4][PtCl6] as precursors for intermetallic compounds PtZn and PtCd. Russ J Inorg Chem. 2007;52:500–4.
5. Yusenko KV, Filatov EY, Vasilchenko DB, Baidina IA, Zadesenez AV, Shubin YV. Synthesis and thermal decomposition of the oxalatho cuprates(II)-[M(NH3)(4)] [Cu(C2O4)(2)]*3H(2)O, M = Pt, Pd. Z Kristallogr. 2007;26(Suppl):289–95.

6. Nashner MS, Somerville DM, Lane PD, Adler DL, Shapley JR, Nuzzo RG. Bimetallic catalyst particle nanostructure. Evolution from molecular cluster precursors. J Am Chem Soc. 1996;118: 12964–74.

7. Gates BC. Supported metal cluster: Synthesis, structure, and catalysis. Chem Rev. 1995;95:511–22.

8. Nashner MS, Frenkel AI, Adler DL, Shapley JR, Nuzzo RG. Structural characterization of carbon-supported platinum-ruthenium nanoparticles from the molecular cluster precursor PtRu$_5$C(CO)$_{16}$. J Am Chem Soc. 1997;119:7760–71.

9. Pocol V, Patrol L, Carp O, Brezeanu M, Segal E, Stanica N, et al. Some polynuclear coordination compounds precursors of chromites: synthesis, physicochemical characterization and thermal stability. J Therm Anal Calorim. 1999;55:143–54.

10. Delmon B. Preparation of heterogeneous catalysts: synthesis of highly dispersed solids and their reactivity. J Therm Anal Calorim. 2007;90:49–65.

11. Bakrania SD, Rathore GK, Wooldridge MS. An investigation of the thermal decomposition of gold acetate. J Therm Anal Calorim. 2009;95:117–22.

12. Lucca Neto VA, Mauro AE, Netto AVG, Moro AC, Noguera VM. Mono and dinuclear Pd(II) complexes pyrazole and imidazole-type ligands. Synthesis, characterization and thermal behavior. J Therm Anal Calorim. 2009;97:57–60.

13. Salavati-Niasari M, Davar F. Synthesis of copper and copper(I) oxide nanoparticles by thermal decomposition of a new precursor. Mater Lett. 2009;63:441–3.

14. Liu X, Lu S, Zhang J, Cao W. Thermal decomposition process of silver behenate. Thermochim Acta. 2006;440:1–6.

15. Boldyrev VV. Thermal decomposition of silver oxalate. Thermochim Acta. 2002;388:63–90.

16. Plyusnin PE, Baidina IA, Shubin YV, Korenev SV. Synthesis, crystal structure, and thermal properties of [Pd(NH$_3$)$_4$][AuCl$_4$]$_2$. Russ J Inorg Chem. 2007;52:371–7.

17. Koningsberger DC, Prins R, editors. X-Ray absorption: principles, applications, techniques of EXAFS, SEXAFS and XANES. New York: John Wiley & Sons; 1988.

18. Crozier ED. A review of the current status of XAFS spectroscopy. Nucl Instrum Methods Phys Res Sect B. 1997;133:134–44.

19. Chernyaeva II. Synthesis of complex compounds of Platinum group metals. Moscow: Nauka; 1964. (in Russian).

20. Ravel B, Newville M. ATHENA, ARTEMIS, HEPHAESTUS: data analysis for X-ray absorption spectroscopy using IFEFFIT. J Synchrotron Rad. 2005;12:537–41.

21. Newville M. IFEFFIT: interactive XAFS analysis and FEFF fitting. J Synchrotron Rad. 2001;8:322–4.

22. Sobczak JW, Sobczak E, Kosiński A, Biliński A. XANES investigations of Pd-doped polyaniline. J Alloys Compd. 2001; 328:132–4.

23. Berrodier I, Farges F, Benedetti M, Winterer M, Brown GE, Deveughele M. Adsorption mechanisms of trivalent gold on iron- and aluminum-(oxy)hydroxides. Part 1: X-ray absorption and Raman scattering spectroscopic studies of Au(III) adsorbed on ferrihydrite, goethite, and boehmite. Geochim Cosmochim Acta. 2004;68:3019–42.

24. Stern EA, Kim K. Thickness effect on the extended-X-ray-absorption-fine-structure amplitude. Phys Rev B. 1981;23:3781–7.